SUPPLEMENTAL FIGURES

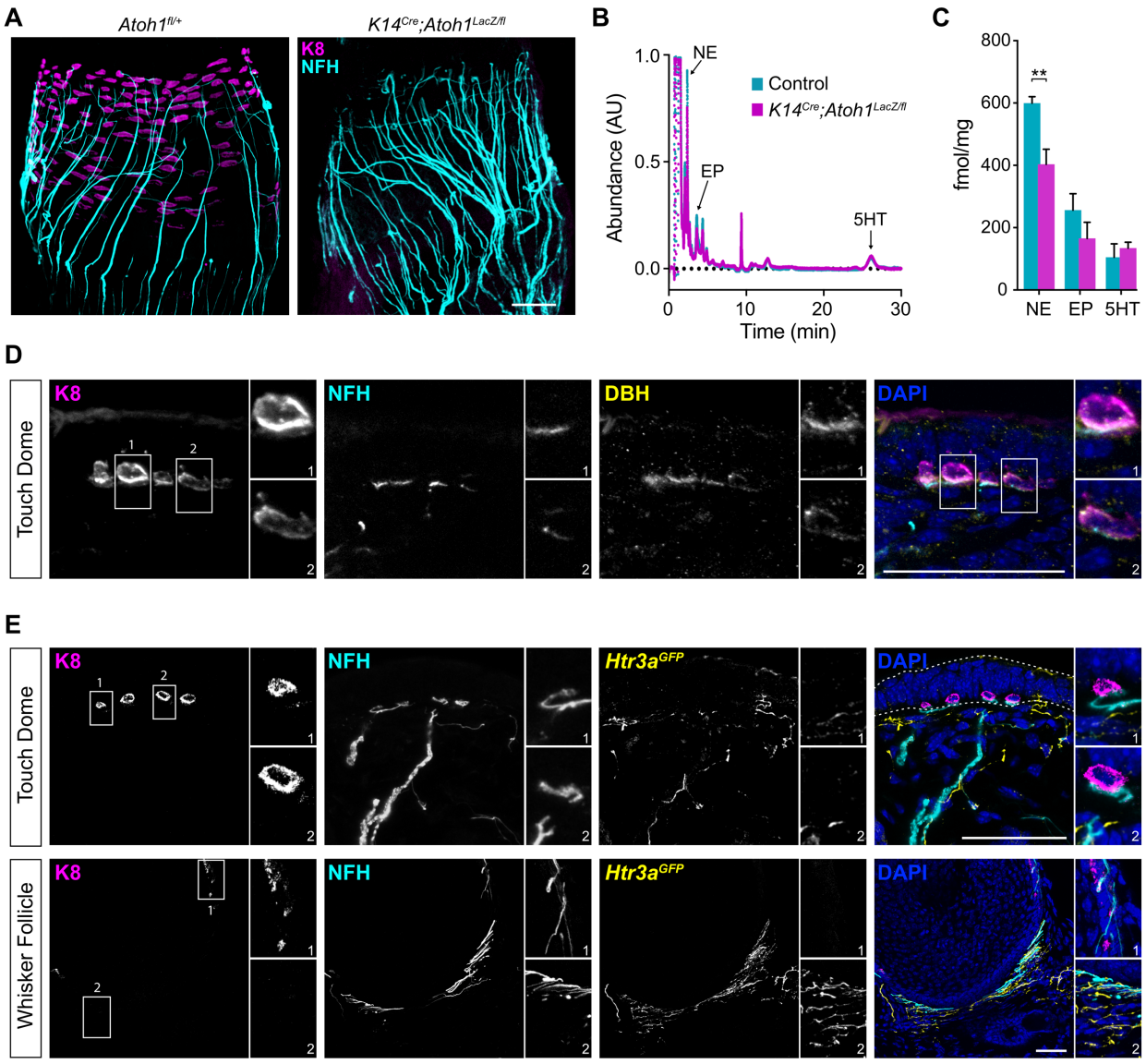

Figure S1. Monoamine neurotransmission at the Merkel cell-neurite complex, related to Figure 1. A. Whole mount immunohistochemistry of micro-dissected whisker follicles from control (*Atoh1*$^{fl/+}$, left) and *K14*^{Cre};*Atoh1*$^{LacZ/fl}$ (right) animals (K8, magenta; NFH, cyan). (**B, C**). HPLC coupled with electrochemical detection of monoamines performed on micro-dissected whisker follicles from control (*Atoh1*$^{fl/+}$ or *Atoh1*$^{LacZ/+}$, cyan) and *K14*^{Cre};*Atoh1*$^{LacZ/fl}$ (magenta) animals (*n*=3 animals per genotype). **B**. Mean traces of HPLC runs by genotype. **C**. Molar amounts, normalized to tissue weight, of norepinephrine (NE), epinephrine (EP), and 5HT (two-way ANOVA with Sidak's post-hoc, **P=0.01; *n*=3 animals per genotype). **(D, E)**. Immunohistochemistry in skin cryosections of touch domes and whisker follicles. Insets show magnified regions indicated by rectangles (1 and 2). **D.** Touch dome immunohistochemistry from a wild-type mouse (K8, magenta; NFH, cyan; DBH, yellow; DAPI, blue). **E.** Immunohistochemistry from touch domes (top) and whisker follicles (bottom) from a mouse expressing $5HT_3$-GFP (K8, magenta; NFH, cyan; $5HT_3$-GFP, yellow; DAPI, blue). Scale bars, 50 µm.

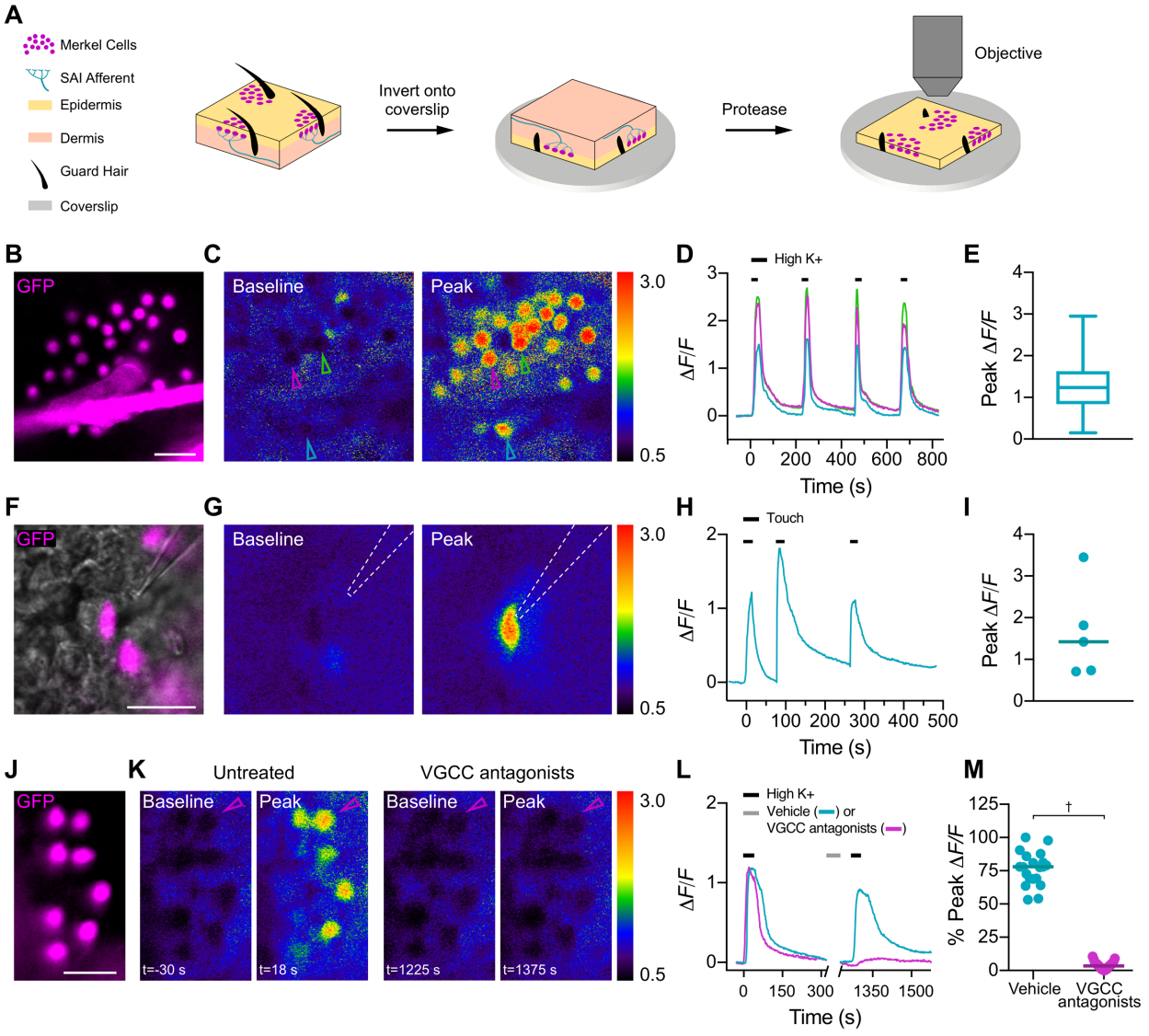

Figure S2. Merkel cells display robust calcium responses to stimulation in a semi-intact epidermal peel preparation, related to Figure 2. (**A**). Schematic of semi-intact epidermal peel preparation. (**B–M**). GFP-positive Merkel cells loaded with Fura-2AM. (**B–D**). Representative Merkel cells (**B**, *Atoh1*^{nGFP}, magenta) depolarized with high K^+ KCl Ringer's solution. **C**. Pseudocolor images representing baseline (left) and peak (right) F_{340}/F_{380} ratios of stimulated Merkel cells. **D**. *ΔF/F* traces of Merkel cells identified by colored arrows in (**C**). Black bars, high K^+ application. **E**. Peak *ΔF/F* data for all responding Merkel cells (*n*=192/207 cells, 2 animals; box, 25th percentile, median, 75th percentile; whisker, min and max). (**F–H**). Representative Merkel cell (**F**, *Atoh1*^{nGFP}, magenta) stimulated with mechanical indentation (**G**, dashed lines, mechanical probe). **H**. *ΔF/F* trace of the Merkel cell in (**G**). Black bars, mechanical indentation. **I**. Peak *ΔF/F* data of mechanically evoked calcium transients in Merkel cells (*n*=5/8 cells, 2 animals; line, median). (**J–L**). Representative Merkel cells (**J**, *Atoh1*^{GFP}, magenta) stimulated with high K^+ before and after incubation with VGCC antagonists (10 μM nimodipine + 10 μM ω-conotoxin MVII-C). **K**. Representative pseudocolor image of Merkel cells stimulated with K^+ in the absence of VGCC antagonists, and Merkel cells stimulated with high K^+ after incubation with VGCC antagonists. **L**. *ΔF/F* traces of a Merkel cell stimulated with K^+ before and after incubation with vehicle (cyan trace), and a Merkel cell stimulated with K^+ before and after incubation with VGCC antagonists (magenta trace; Merkel cell in **K**, magenta arrow). Black bars, K^+ application. Gray bars, incubation with vehicle or VGCC antagonists. **M**. Peak *ΔF/F* after treatment (vehicle or control) normalized to peak *ΔF/F* before treatment (% peak *ΔF/F*) for all Merkel cells (two-tailed t-test, †P<0.0001. *n*=21-22 cells per group from one animal; lines denote means). Scale bars, 20 μm. See also Movies S1, S2.

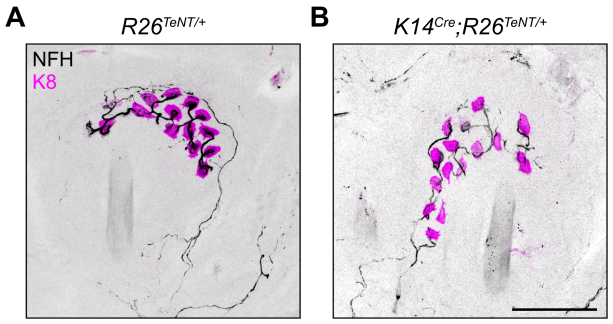

Figure S3. Touch domes from *R26*$^{TeNT+}$ and *K14*^{Cre}*;R26*$^{TeNT+}$ mice showed innervated Merkel-cell clusters, related to Figure 3. (**A, B**). Whole-mount immunohistochemistry and confocal axial projection of touch domes from *R26*$^{TeNT+}$ (**A**) and *K14*^{Cre}*;R26*$^{TeNT+}$ (**B**) mice. Scale bar, 50 μm.

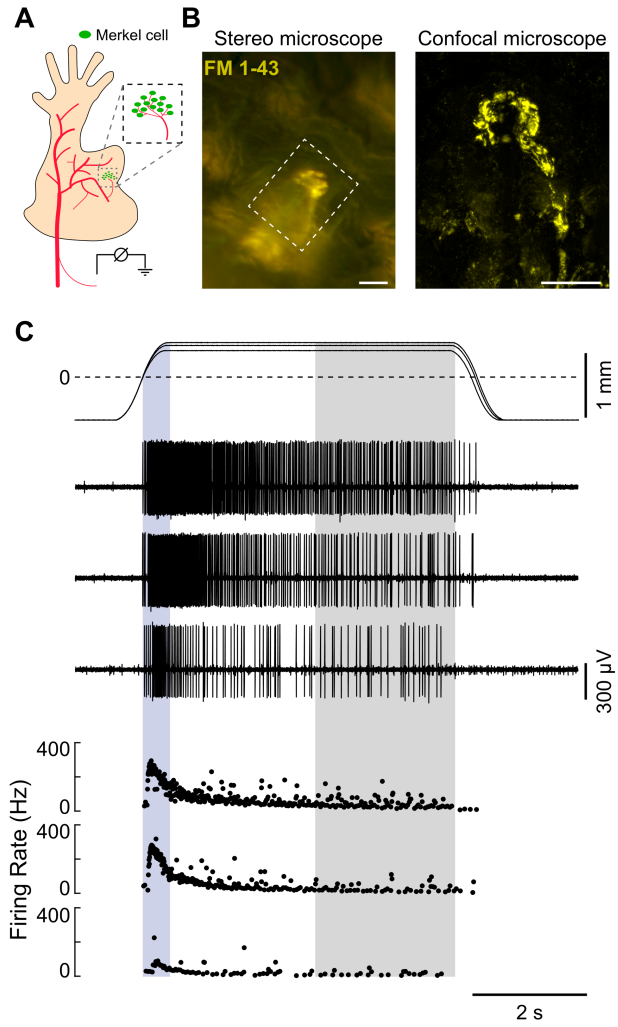

Figure S4. *Ex vivo* skin-saphenous nerve single-unit recordings from fluorescently labeled touch-dome afferents, related to Figure 3. A. Schematic of experimental setup. Hind limb skin was dissected with innervation from the saphenous nerve (red) maintained intact. Touch domes were identified by *in vivo* injection with FM 1-43, which labels Merkel cells (green) and sensory neurons. Neuronal responses from teased fibers are recorded with a differential electrode. **B**. Representative image of a FM 1-43 labeled touch dome (box) visualized with a stereo microscope (left) and a confocal microscope (right; scale bars, 50 µm). **C**. Representative skin-nerve recording of a fluorescently identified touch-dome afferent. Top traces depict displacements (dashed lines: point of skin contact). Middle traces depict resulting neuronal action potential trains (in descending stimulus magnitude). Corresponding instantaneous firing frequency (IFF) plots shown on the bottom (blue shaded region, dynamic phase of stimulation; gray shaded region, static phase of stimulation).

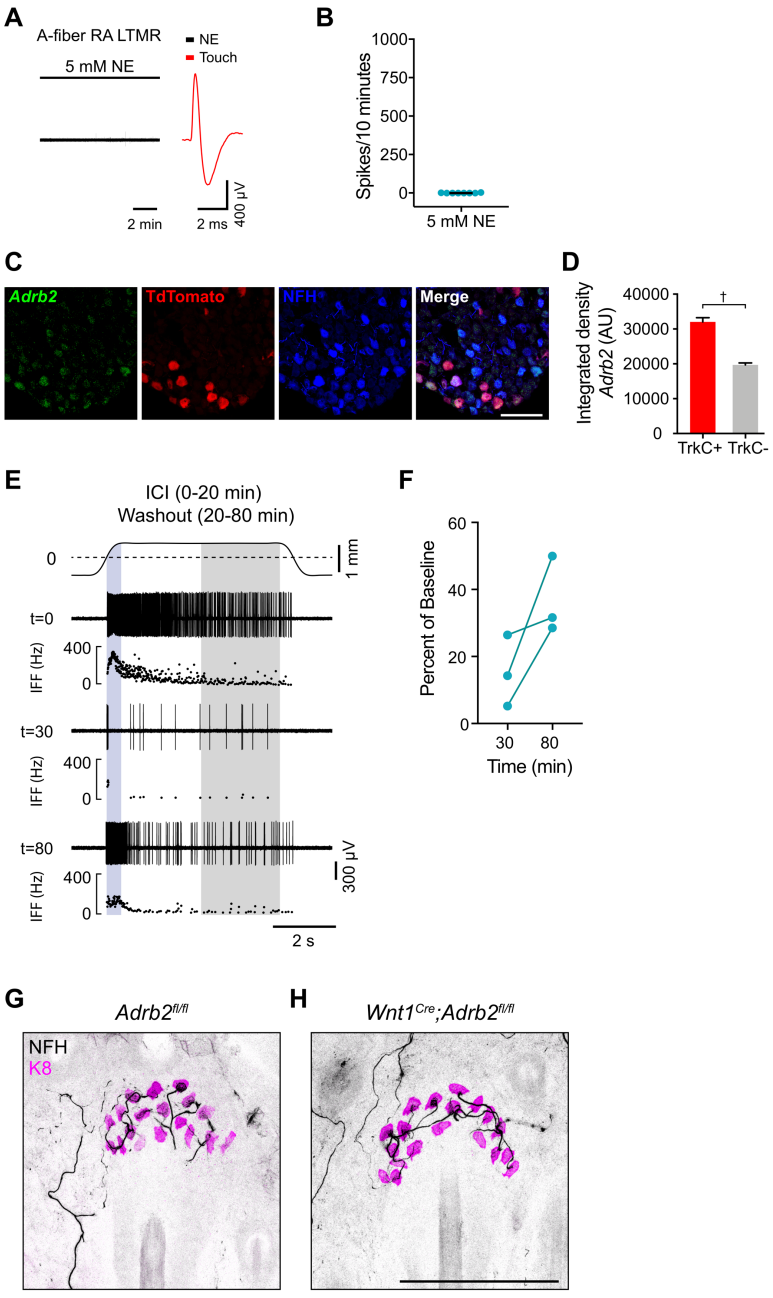

Figure S5. Adrenergic signaling in touch receptors, related to Figure 5. (**A, B**). Norepinephrine (5 mM) was applied to receptive fields of A-fiber RA-LTMRs in dermis-side up skin-nerve recordings. **A.** Left, representative trace. Right, touch-evoked action potential waveform (red). Black bar, norepinephrine application (10 min). **B.** Total spikes evoked by norepinephrine in A-fiber RA-LTMRs (n=8 fibers, 4 mice; line, median=0). **C.** Representative confocal images of single molecule *in situ* hybridizations (probe targeting the β_2AR, *Adrb2*, green) and immunohistochemistry (antibody to label TrkC^{tdtomato} neurons, TdTomato, red; NFH, blue) performed on cryosections of adult DRG (25 µm). **D**. Quantification of hybridization integrated density measurements (Mann-Whitney test, $^{\dagger}P<0.0001$; n_{TrkC+}=541, n_{TrkC-}=905 neurons, 2 mice; mean±SEM). **E.** Representative experiment of touch-evoked firing from a Merkel-cell afferent that showed recovery after washout of 50 µM ICI 118,551 (ICI). ICI was applied from 0-20 minutes, and washout was from 20-80 minutes. Traces and shading as in **Fig. 5B. F.** Baseline normalized mean firing rates during static stimulation of Merkel-cell afferents stimulated 30 min after and 80 min after treatment with 50 µM ICI. In all recordings that lasted >80 minutes (3/6 ICI recordings), static firing showed partial recovery after 60 min of ICI washout. (**G, H**). Whole-mount staining and confocal axial projection of touch domes from *Adrb2*$^{fl/fl}$ (**G**) and *Wnt1*^{Cre};*Ardb2*$^{fl/fl}$ (**H**) mice. Scale bars, 100 µm.

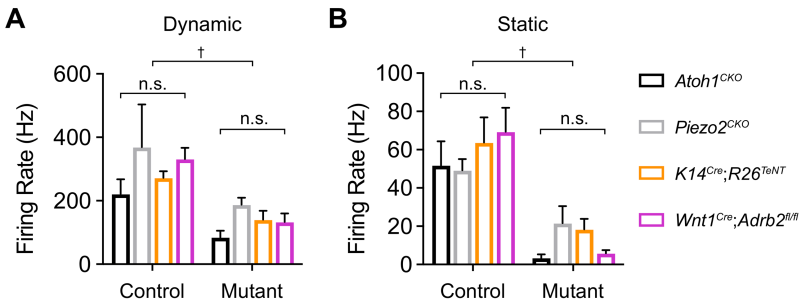

Figure S6. Merkel cells enhance the excitability of Aβ LTMRs during dynamic touch stimuli and mediate mechanosensory responses to gentle pressure, related to Figure 6. (**A, B**). Comparison of maximum touch-evoked responses from touchdomes in *Atoh1*-knockout (black), *Piezo2*-knockout (gray), *K14*^{Cre};*R26*^{TeNT} (orange; from **Fig. 3C–F**), and *Wnt1*^{Cre};*Adrb2*$^{fl/fl}$ (magenta; from **Fig. 5G–I**), and littermate control mice (Maksimovic et al., 2014; Woo et al., 2014). **A.** Peak firing rates during the dynamic phase of stimulation. **B.** Mean firing rates during the static phase of stimulation (two-way ANOVA, Sidak's post-hoc, $^{\dagger}P<0.0001$; errors, mean±SEM).

SUPPLEMENTAL TABLE

Table S3. Characteristics of fibers from *ex vivo* recordings, related to Figures 3, 4, 5, S4 and S5.

Figure	Fiber ID	Sex	Age (days)	Genotype	CV (m/s)	von Frey (mN)	Fiber type
3C, D	1	F	66	$R26^{TeNT/+}$	15.2	0.08	SAI
3C, D	2	M	67	$R26^{TeNT/+}$	15.5	0.08	SAI
3C, D	3	F	56	$R26^{TeNT/+}$	17.4	0.08	SAI
3C, D	4	M	80	$R26^{TeNT/+}$	13.8	0.20	SAI
3C, D	5	M	80	$R26^{TeNT/+}$	19.0	0.08	SAI
3C, D	6	F	55	$R26^{TeNT/+}$	18.4	0.08	SAI
3C, D	7	M	57	$R26^{TeNT/+}$	15.6	0.20	SAI
3C, D	8	M	81	$R26^{TeNT/+}$	17.2	0.08	SAI
3C, D	9	F	81	$R26^{TeNT/+}$	18.0	0.20	SAI
3C, D; S4A–C	10	F	82	$R26^{TeNT/+}$	21.2	0.08	SAI
3C, D	11	F	73	$K14^{Cre};R26^{TeNT/+}$	15.7	0.08	SAI
3C, D	12	F	62	$K14^{Cre};R26^{TeNT/+}$	16.1	0.08	SAI
3C, D	13	F	62	$K14^{Cre};R26^{TeNT/+}$	16.7	0.20	SAI
3C, D	14	M	64	$K14^{Cre};R26^{TeNT/+}$	15.1	0.08	SAI
3C, D	15	M	64	$K14^{Cre};R26^{TeNT/+}$	19.4	0.20	SAI
3C, D	16	M	69	$K14^{Cre};R26^{TeNT/+}$	15.9	0.08	SAI
3C, D	17	F	69	$K14^{Cre};R26^{TeNT/+}$	18.9	0.20	SAI
3C, D	18	M	51	$K14^{Cre};R26^{TeNT/+}$	16.4	0.08	SAI
3C, D	19	F	55	$K14^{Cre};R26^{TeNT/+}$	18.4	0.08	SAI
3C, D	20	M	56	$K14^{Cre};R26^{TeNT/+}$	17.4	0.08	SAI
3C, D	21	F	94	$K14^{Cre};R26^{TeNT/+}$	22.0	0.08	SAI
4A–C	22	F	49	WT	14.5	0.08	SAI
4A–C	23	F	50	WT	14.3	0.08	SAI
4A–C	24	F	50	WT	17.8	0.08	SAI
4A–C	25	F	51	WT	18.9	0.20	SAI
4A–C	26	F	51	WT	17.6	0.08	SAI
4A–C	27	F	63	WT	12.5	0.20	SAI
4A–C	28	F	63	WT	11.2	0.08	SAI
4A–C	29	F	63	WT	13.7	0.08	SAI
4A–C	30	F	55	WT	16.0	0.08	SAI
4A–C	31	F	55	WT	11.2	0.08	SAI
4A–C	32	F	56	WT	12.7	0.08	SAI
4A–C	33	F	61	WT	13.2	0.20	SAI
4A–C	34	F	62	WT	16.1	0.08	SAI
4A–C	35	F	63	WT	11.0	0.20	SAI
4A–C	36	F	69	WT	13.5	0.08	SAI
4A–C	37	F	53	WT	11.1	0.08	SAI
4A–C	38	F	59	WT	10.5	0.08	SAI

4A–C	39	F	60	WT	9.6	0.08	SAI
5B–F	40	F	57	WT	13.1	0.08	SAI
5B–F	41	F	58	WT	17.3	0.08	SAI
5B–F	42	F	62	WT	13.0	0.08	SAI
5B–F	43	F	63	WT	12.3	0.08	SAI
5B–F	44	F	64	WT	12.8	0.08	SAI
5B–F	45	F	70	WT	13.6	0.08	SAI
5B–F	46	F	51	WT	15.5	0.08	SAI
5B–F; S5E, F	47	F	56	WT	14.9	0.20	SAI
5B–F	48	F	51	WT	11.5	0.08	SAI
5B–F	49	F	56	WT	12.7	0.20	SAI
5B–F	50	F	58	WT	13.2	0.08	SAI
5G–J	51	F	69	*Adrb2*$^{fl/fl}$	10.7	0.08	SAI
5G–J	52	M	90	*Adrb2*$^{fl/fl}$	15.8	0.20	SAI
5G–J	53	M	91	*Adrb2*$^{fl/fl}$	13.3	0.08	SAI
5G–J	54	M	60	*Adrb2*$^{fl/fl}$	13.6	0.20	SAI
5G–J	55	M	73	*Adrb2*$^{fl/fl}$	11.6	0.08	SAI
5G–J	56	F	81	*Adrb2*$^{fl/fl}$	15.8	0.08	SAI
5G–J	57	M	94	*Adrb2*$^{fl/fl}$	13.4	0.20	SAI
5G–J	58	F	86	*Adrb2*$^{fl/fl}$	17.4	0.08	SAI
5G–J	59	F	86	*Adrb2*$^{fl/fl}$	14.0	0.08	SAI
5G–J	60	M	59	*Adrb2*$^{fl/fl}$	13.1	0.08	SAI
5G–J	61	F	61	*Wnt1*^{Cre};*Ardb2*$^{fl/fl}$	10.8	0.20	SAI
5G–J	62	F	92	*Wnt1*^{Cre};*Ardb2*$^{fl/fl}$	15.9	0.08	SAI
5G–J	63	F	92	*Wnt1*^{Cre};*Ardb2*$^{fl/fl}$	12.4	0.20	SAI
5G–J	64	F	65	*Wnt1*^{Cre};*Ardb2*$^{fl/fl}$	13.4	0.08	SAI
5G–J	65	F	65	*Wnt1*^{Cre};*Ardb2*$^{fl/fl}$	10.8	0.20	SAI
5G–J	66	M	74	*Wnt1*^{Cre};*Ardb2*$^{fl/fl}$	15.2	0.20	SAI
5G–J	67	M	80	*Wnt1*^{Cre};*Ardb2*$^{fl/fl}$	12.0	0.20	SAI
5G–J	68	F	85	*Wnt1*^{Cre};*Ardb2*$^{fl/fl}$	15.5	0.08	SAI
5G–J	69	M	63	*Wnt1*^{Cre};*Ardb2*$^{fl/fl}$	11.2	0.08	SAI
S5A, B	70	F	53	WT	10.2	0.20	A-fiber RA LTMR
S5A, B	71	F	53	WT	10.7	0.08	A-fiber RA LTMR
S5A, B	72	F	57	WT	10.4	0.20	A-fiber RA LTMR
S5A, B	73	F	58	WT	9.7	0.08	A-fiber RA LTMR
S5A, B	74	F	58	WT	10.1	0.20	A-fiber RA LTMR
S5A, B	75	F	59	WT	11.1	0.08	A-fiber RA LTMR
S5A, B	76	F	59	WT	10.0	0.08	A-fiber RA LTMR
S5A, B	77	F	59	WT	9.0	0.08	A-fiber RA LTMR